Published online 20 February 2007

Nucleic Acids Research, 2007, Vol. 35, No. 5 ***1687–1697***
doi:10.1093/nar/gkl1141

Ovol1 represses its own transcription by competing with transcription activator c-Myb and by recruiting histone deacetylase activity

Mahalakshmi Nair[1,2], Virginia Bilanchone[1], Kori Ortt[3], Satrajit Sinha[3] and Xing Dai[1,2,*]

[1]Department of Biological Chemistry, School of Medicine, [2]Developmental Biology Center, University of California, Irvine, CA 92697, USA and [3]Department of Biochemistry, State University of New York at Buffalo, New York, USA

Received October 30, 2006; Revised December 13, 2006; Accepted December 14, 2006

ABSTRACT

Ovol1 belongs to a family of evolutionarily conserved zinc finger proteins that act downstream of key developmental signaling pathways such as Wnt and TGF-β/BMP. It plays important roles in epithelial and germ cell development, particularly by repressing c-Myc and Id2 genes and modulating the balance between proliferation and differentiation of progenitor cells. In this study, we show that Ovol1 negatively regulates its own expression by binding to and repressing the activity of its promoter. We further demonstrate that Ovol1 uses both passive and active repression mechanisms to auto-repress: (1) it antagonizes transcriptional activation of c-Myb, a known positive regulator of proliferation, by competing for DNA binding; (2) it recruits histone deacetylase activity to the promoter via an N-terminal SNAG repressor domain. At Ovol1 cognate sites in the endogenous *Ovol1* promoter, c-Myb binding correlates with increased histone acetylation, whereas the expression of Ovol1 correlates with a displacement of c-Myb from the DNA and decreased histone acetylation. Collectively, our data suggest that Ovol1 restricts its own expression by counteracting c-Myb activation and histone acetylation of the *Ovol1* promoter.

INTRODUCTION

The evolutionarily conserved *ovo* genes encode C_2H_2 zinc finger transcription factors and act downstream of Wg(Wnt)/β-catenin and TGF-β/BMP signaling pathways that have been widely implicated in normal and malignant development of myriad tissues (1,2). Functional studies in several organisms have demonstrated an involvement of *ovo* genes in the development and differentiation of a number of epithelial lineages (2–7). However, less progress has been made on the biochemical mechanism by which Ovo proteins function to regulate gene expression in these biological processes.

Ovol1 is expressed in the epithelial tissues of hair follicles, interfollicular epidermis, kidney, as well as in the male germinal epithelium (7). In these tissues, *Ovol1* expression correlates with the onset of terminal differentiation of progenitor cells (7–9). *Ovol1* knockout mice display pleiotropic defects including ruffled hairs, a hyperproliferative epidermis, defective spermatogenesis and cystic kidneys (7–10). A common theme of *Ovol1* function appears to be promoting the transition from a proliferating, less differentiated state to a post-mitotic, more differentiated state. In epidermis, *Ovol1* is required for embryonic epidermal progenitor cells to efficiently exit proliferation to embark on the terminal differentiation process (9). During spermatogenesis, *Ovol1* is required for germ cells to exit from mitosis and enter meiosis (8). *Ovol1* likely plays a similar role in kidney epithelial cells, as it is known that over-proliferation of these cells results in kidney cyst formation (11). Three downstream targets of Ovol1 have been identified: c-Myc, Id2 and *Ovol2* (8–10). These genes are expressed in proliferating progenitor cells and their expression is up-regulated when *Ovol1* is deleted. Both c-Myc and Id2 are known to have pro-proliferation and/or anti-differentiation roles, and therefore their negative regulation by Ovol1 is consistent with the growth inhibitory function of Ovol1 (8,9).

Feedback control is common for important regulators of development. Genetic evidence suggests that *Drosophila ovo* auto-regulates (12,13), underlying the importance of an intricate regulation of *ovo* gene expression. This raises the interesting possibility that *Ovol1* might be a target of transcriptional repression by its own gene product. Distinct from *Drosophila ovo* and mouse *Ovol2*, which encode multiple protein isoforms with either transcriptional activator or repressor activity (14–16), *Ovol1* encodes a single polypeptide with

*To whom correspondence should be addressed. Tel: +1 949 824 3101; Fax: +1 949 824 2688; Email: xdai@uci.edu

transcriptional repressor activity (7–9). In this study, we address whether Ovol1 represses its own expression and how it represses transcription at a mechanistic level.

The predominant mode of action of a sequence-specific DNA-binding transcriptional repressor in eukaryotes is to recruit co-repressor complexes to its target promoters (active repression). Many sequence-specific repressors recruit histone deacetylases (HDACs), either directly or via adaptor proteins such as Sin3 [reviewed in (17,18)]. HDACs, opposing the function of histone acetylases, catalyze the deacetylation of lysine residues of core histone tails. This results in a more compact chromatin structure and consequently decreased accessibility for transcription factors. Two of the class I HDACs, HDAC1 and HDAC2, have been most widely implicated in transcriptional repression by myriad DNA-binding repressors (19). Transcriptional repression can also occur by a passive mechanism, where repressors interfere with the function of transcriptional activators, for example by competing for binding to common DNA sequences [reviewed in (18,20)]. Does Ovol1 interact biochemically or functionally with such repressors or activators? Such insight will add to our overall understanding of molecular pathways underlying the control of epithelial cell proliferation and differentiation, and might implicate additional potential players in this important process. Here we provide evidence that Ovol1 negatively regulates its own expression by binding to and repressing the *Ovol1* promoter. We further demonstrate that Ovol1 represses transcription using both passive (competing with the c-Myb transcriptional activator, a known positive regulator of proliferation) and active (recruiting HDAC1) repression mechanisms.

MATERIALS AND METHODS

CASTing (cyclic amplification of selected targets)

An 80-bp oligonucleotide was synthesized (IDT Technologies), which contained 35-base random nucleotides flanked by sequences complementary to primers A and B for cloning purposes. The sequences of these three oligonucleotides are as follows: 80-base oligonucleotide, 5′-GGATCCCTGCCTTCACCGAAGC$(N)_{35}$TTGGGG ACTATGAATTCCTGAGG-3′; primer A, 5′-GGATCC CTGCCTTCACCGAAG-3′; primer B, 5′-CCTCAGGA ATTCATAGTCCCC-3′. A random sequence library of double-stranded radiolabeled oligonucleotides was prepared by annealing the 80-base oligonucleotide to 5-fold molar excess of primer B followed by extension with Klenow. The extension reaction for the annealed double-stranded oligonucleotide was performed in 50 µl of the labeling reaction mixture that contained 50 mM Tris-HCl (pH 7.5), 10 mM $MgCl_2$, 100 µM each of dATP, dGTP and dTTP and 5 µl of 3000 Ci/nmol of [α-^{32}P]-dCTP. The labeling reaction mixture was incubated at 37°C for 1 h with 5 units of the Klenow enzyme (Stratagene). The radiolabeled DNA was purified by using G-50 Nick columns (Amersham) and subjected to EMSA. EMSAs were performed by adding 100 ng of recombinant His_6–Ovol1 protein (9) to DNA-binding buffer (5% glycerol, 10 mM HEPES, pH 7.9, 75 mM KCl, 1 mM DTT, 2.5 mM $MgCl_2$, 1 mM EDTA, 1 mM $ZnCl_2$) containing 0.5 µg of poly (dA.dT), 5 µg of bovine serum albumin, and 10 fmols of ^{32}P-labeled probe. The reaction was incubated at room temperature for 30 min and the DNA–protein complexes were resolved by electrophoresis through a non-denaturing 5% polyacrylamide gel in 1×Tris-borate-EDTA (TBE) buffer at 100 V for 3 h. The complexes specifically formed in the presence of His_6–Ovol1 were detected by autoradiography, excised from gels, and eluted overnight at 37°C in DNA-elution buffer containing 0.3 M NaCl, 1 mM EDTA and 0.1% SDS. The eluted DNA was extracted once in phenol–chloroform, and then precipitated with ethanol. The purified DNA was subjected to PCR amplification with primers A and B in the presence of [α-^{32}P]-dCTP. Amplification was carried out by 20 cycles of denaturation at 94°C for 20 s, annealing at 49°C for 20 s and extension at 72°C for 30 s. The amplified DNA was purified using G-50 Nick columns, and was used in subsequent EMSA experiments. After four cycles of CASTing, the final amplified DNA was cloned directly using pCR2.1-TOPO TA Cloning kit (Invitrogen). Nucleotide sequences of 105 independent clones were determined. The degenerate portion of the sequences was compiled and analyzed for shared sequence patterns by matrix-based pattern discovery using the CONSENSUS program developed by Jerry Hertz (web interface by Jacques van Helden; http://rsat.ulb.ac.be/rsat).

Electrophoretic mobility shift assay (EMSA)

The full-length and truncated Ovol1 proteins used for EMSA assays were produced in bacteria (9) or by *in vitro* transcription/translation reactions. Briefly, 5 µg of the linearized DNA template for the transcription reaction was generated by digesting the appropriate expression plasmids overnight at 37°C with BamHI. The linearized DNA was then phenol-chloroform extracted and ethanol precipitated. One microgram of the linearized DNA was next incubated in 50 µl of transcription mix containing 10 mM DTT, 1 mM rNTPs, 40 units of RNase inhibitor RNAout (Promega) and T7 RNA polymerase for 1 h at 37°C. The transcribed RNA was isolated by phenol–chloroform extraction and ethanol precipitation. A portion of this RNA (3 µl of the 50 µl transcription reaction) was next used in *in vitro* translation reaction containing ^{35}S-methionione to generate ^{35}S-labeled proteins. The translation reaction was performed in a 20-µl reaction volume using the rabbit reticulocyte lysate system (Promega, Cat # L4960), exactly as per manufacturer's instructions. One microliter of the translation reaction was thereafter run on a 10% SDS-PAGE gel and autoradiographed to ensure the generation of ^{35}S-labeled protein products of the appropriate molecular weights

for the various expression constructs. The 12 kDa R2R3 DNA-binding domain of chicken c-Myb was generated as described (21,22), and used in the DNA-binding studies because it displays a much higher affinity for cognate sites than the full-length protein (23). EMSA was performed as described using 0.2–0.3 pmol of labeled oligonucleotides and 0.05–2.5 μg of recombinant His_6–Ovol1, or 1–3 μl of the 20-μl translation reaction, or 1.5–3 μg of c-Myb-expressing bacterial extracts. The sequences of c-Myb cognate oligonucleotides mim-A and mim-C are 5′-AGCGCTAAAAAACCGTTATAATGTGCA GAT-3′ and 5′-GTTGATTTCCATCTGTTATTTGAG CTAAG-3′, respectively. The protein–DNA complexes were resolved on 6% non-denaturing polyacrylamide gels and visualized by autoradiography.

DNase I and hydroxyl radical footprinting

DNase I footprinting assay was performed using a Sau3AI–BssHII fragment (position −356 to +15) of the *Ovol1* promoter, labeled with ^{32}P at the Sau3AI end and 0.5–3 μg of recombinant His_6–Ovol1 protein as described in (1). The Maxim–Gilbert reactions G, C and C + T were used as molecular-weight markers. Hydroxyl radical footprinting assay was performed as described (24) in a volume of 200 μl containing 20–30 fmol ($\sim 4 \times 10^4$ cpm) of 5′ P^{32} single end-labeled Ovol1 promoter fragment (position −356 to +15) and 0.5–2 μg of recombinant His_6–Ovol1 protein. Specifically, protein–DNA binding was for 20 min at room temperature, followed by treatment with hydroxyl radical for 5 min at room temperature, and finally quenched by the addition of 20 μl of 0.2 M thiourea. Reaction products were resolved by electrophoresis on a 10% denaturing polyacrylamide gel containing 7 M urea in TBE buffer along with Maxim–Gilbert G, C and C + T reactions on the same promoter fragment. Gels were scanned by a phosphorimager and band intensities quantified.

Northern blot analysis

Total RNA was extracted from skin of *Ovol1*$^{-/-}$ embryos and control littermates, and northern analysis was performed as described using an *Ovol1* probe that hybridizes to a 1-kb region at the 5′of the cDNAs (7).

Reporter assays

Assays were performed in 293T and NIH3T3 cells. The 293T cells were transfected using calcium phosphate as described (25) and NIH3T3 cells using Polyfectene (Qiagen). Typically, transfection experiments were done in 24-well plates with each well transfected with a total of 0.5 μg of plasmids including 0.05 μg of pGL3-*Ovol1* [where *Ovol1* promoter is cloned upstream of the luciferase reporter; (1)] or 0.02 μg of Gal-tk-luc (where luciferase is under the control of a minimal tk promoter downstream of Gal4-binding sites, or tk-luc control), 0.04 μg of β-actin-β-gal construct (transfection control), varying amounts of Ovol1 expression constructs (as indicated in figure legends), and murine c-Myb expression vector (pEQP2-CMV-c-Myb) wherever mentioned. pCB6+ or pCMX-GalDBD (empty vector containing the CMV promoter) was used as filler DNA. In these and subsequent experiments, the amounts of wild-type and mutant expression plasmids were standardized based on quantification of protein levels by Western blot analysis. Cells were harvested 48–60 h after transfection and luciferase activity was measured in whole cell extracts using the Luciferase Assay System (Promega). β-galactosidase activity was measured as previously described (26). Transfection assay to study the effect of the HDAC inhibitor trichostatin A (TSA) was performed by adding TSA ~ 28 h after transfection at a final concentration of 100 ng/ml. Cells were collected 20 h later for luciferase and β-galactosidase analyses.

Immunoprecipitation (IP)

IP experiments were done using whole cell lysates from 293T cells seeded in 10-cm dishes and transfected with 8 μg of pCB6-Ovol1 (or 1.6 μg of Δ15-Ovol1, in which the first 15 amino acids were deleted) and 14 μg of Flag-tagged HDAC1, −2 or −3 (generous gifts of Dr Edward Seto, H. Lee Moffitt Cancer Center and Research Institute). To detect the interaction between Ovol1 and endogenous HDAC1, 293T cells transfected with 6 μg of pCB6-Ovol1 were used. IP was performed as described (27) using anti-Flag (Cat # F3165, Sigma) or anti-Ovol1 (1) antibodies. Western blots were probed with anti-Flag, anti-Ovol1, anti-HDAC1 (Cat #sc-7872, Santa Cruz), or anti-HDAC3 (Cat # 05-813, Upstate) antibodies.

Chromatin immunoprecipitation (ChIP)

NIH3T3 cells plated in 10-cm dishes were transfected with either 8 μg pCB6-Ovol1 (or 8 μg Δ15), or 4 μg pCB6-Ovol1 (or 4 μg ZnFC2A) and 8 μg of a murine c-Myb expression construct, or 8 μg of the c-Myb expression construct. Immunoprecipitation was performed per instructions from Upstate using anti-Ovol1, anti-c-Myb (Cat #sc-7874, Santa Cruz), anti-acetyl histone H3 (Cat # 06-599, Upstate) or anti-HDAC1 antibodies. The immunoprecipitates were analyzed by semi-quantitative PCR using the following primer pairs: 2F: 5′-GAAACCGG TTCGACAGGTAAC-3′ and 2R: 5′-TTTCCAACTAC GCCGAAGGTC-3′; 1F: 5′-ACTCACAGAGCTACACC TGCCT-3′ and 1R: 5′-CATGTGTTCCTGGTCCTTGA G-3′. Select samples were also analyzed by real-time PCR (data not shown). The PCR program used was: 94°C, 1 min, followed by 30–33 cycles of 94°C, 45 s; 60°C, 45 s; 72°C, 1 min and a final extension at 72°C for 7 min. The ChIP signal for a given primer pair was computed as a ratio of the difference in PCR band intensity between the specific antibody and control IgG over the PCR band intensity of the input sample prior to immunoprecipitation.

RESULTS

Ovol1 binds to its own promoter

A thorough understanding of the DNA sequence determinants of Ovol1 binding is an important prerequisite for studies of its downstream targets and transcriptional regulatory activity. Previous analysis of several mouse genomic DNA sequences to which Ovol1 binds *in vitro* led to the identification of a CCGTTA sequence as a likely Ovol1 recognition motif (9). To further define high-affinity Ovol1-binding consensus, we employed CASTing (Cyclic Amplification of Selected Targets), a non-biased, *in vitro* site-selection approach. This analysis identified a 10-bp consensus sequence, A/TA/TA/TCC/TGTTAA/T, that was bound by recombinant Ovol1 (Table 1). This consensus strongly resembles the *Drosophila* OVO recognition sequence ACMGTTACT (M = A, C, T) (28). While the core hexamer, CC/TGTTA, is almost identical to the previously obtained motif, it is clear that high-affinity Ovol1 sites favor flanking sequences that are AT-rich.

To test the utility of our CASTing-identified consensus and based on the finding that *Drosophila ovo* locus is auto-regulatory (12,13), we searched the *Ovol1* promoter for presence of this consensus motif. Care was taken to look for putative sites that have AT-rich flanking sequences. Two such sequences were found in the 700-bp *Ovol1* promoter (1) (Figure 1A), both close to the transcription start site (+1), reminiscent of a key feature of the *Drosophila* OVO-binding sites (29). The proximal site (*Ovol1D*) is a better match to the consensus than the distal one (*Ovol1L*), and consistently *Ovol1D* bound Ovol1 with a higher apparent affinity than *Ovol1L* (Figure 1B). The specificity of the interaction was confirmed by the observation of a supershift of the Ovol1–DNA complex when anti-Ovol1 antibody was added (lane 9, Figure 1B). These results indicate that the sequence parameters revealed by the CASTing analysis can be used to identify *bona fide* Ovol1-binding sites in natural promoters.

To further characterize the Ovol1–*Ovol1* promoter interaction, we performed two additional lines of experiments. First, we generated recombinant proteins containing only the C-terminal (amino acids 107–267, including the zinc finger domain) or the N-terminal half (amino acids 1–107, lacking the zinc finger domain) of Ovol1 and tested their ability to bind to *Ovol1D*. The C-terminal half retained the ability to bind but the N-terminal half did not (Figure 1C), indicating that the DNA-binding moiety of Ovol1 is the zinc finger domain. Second, we performed footprinting experiments using a 370-bp *Ovol1* promoter fragment (corresponding to −356 to +15 bp) encompassing both the proximal and distal Ovol1-binding sites to determine the nucleotide contacts of Ovol1 in a large sequence context. Under the experimental conditions used, increasing concentrations of recombinant Ovol1 created a single DNase I footprint of ~19 bp encompassing the proximal but not the distal site (in bracket) (Figure 1D). This result confirms that the proximal sequence constitutes a higher-affinity site. Hydroxyl radical, a small chemical reagent that cleaves DNA in a base-independent manner, was next employed to pinpoint the nucleotides within this region that contact Ovol1. Footprinting with hydroxyl radical usually provides a finer mapping of protein–DNA contacts due to the small size of the reagent and hence greater accessibility to DNA. The result of this experiment confirmed that Ovol1 makes contacts with the core hexamer, CCGTTA (Figure 1E), within the DNase I-footprinted region of the *Ovol1* promoter. In addition, a 5-bp sequence, GTTGT (or CAACA, opposite strand, underlined in Figure 1E), which is slightly upstream of the hexamer, was also contacted by Ovol1. Together, these results identify the *Ovol1* promoter as a putative target of Ovol1 and provide new insights into how Ovol1 interacts with DNA.

Table 1. A weighted matrix to determine the Ovol1 consensus binding site.

Position	−3	−2	−1	1	2	3	4	5	6	7
(Percent Occurrence) A	46	43	51	22	10	0	6	0	72	33
(Percent Occurrence) C	7	11	8	56	46	0	16	0	8	11
(Percent Occurrence) G	18	15	10	3	0	100	0	2	12	17
(Percent Occurrence) T	29	31	31	19	44	0	78	98	8	39
Ovol1 Consensus site	A/T	A/T	A/T	C	C/T	G	T	T	A	A/T

Ovol1 represses the transcription of its own promoter in a DNA binding-dependent manner

We performed both *in vivo* and *in vitro* experiments to examine whether Ovol1 regulates its own transcription. *Ovol1* knockout mice, in which exons 3 and 4 encoding the C-terminal zinc finger region are deleted, produce no detectable Ovol1 protein (1) but still generate aberrant, high-molecular-weight transcripts (7). The first two exons of the gene as well as the upstream regulatory sequences (including the Ovol1-binding sites identified above) remain intact in these mutant animals, therefore allowing us to compare the total level of transcripts generated from the wild-type and mutant *Ovol1* alleles to assess auto-regulation. Northern blot analysis of skin RNAs isolated from wild-type and $Ovol1^{-/-}$ newborns and E16.5 embryos revealed significantly higher transcript levels in the mutant (Figure 2A and data not shown). This result suggests that transcription from the *Ovol1* locus is up-regulated when Ovol1 protein is absent.

We next performed reporter assays to directly assess the effect of Ovol1 protein on *Ovol1* promoter activity. In 293T cells, a dosage-dependent repression of the basal activity of the promoter by Ovol1 was observed (Figure 2B). A similar repression was observed in NIH3T3 cells, although there the basal promoter activity was significantly lower (data not shown). The repression depended on the ability of Ovol1 to bind to DNA, as mutating the cysteines in the first three C_2H_2 zinc

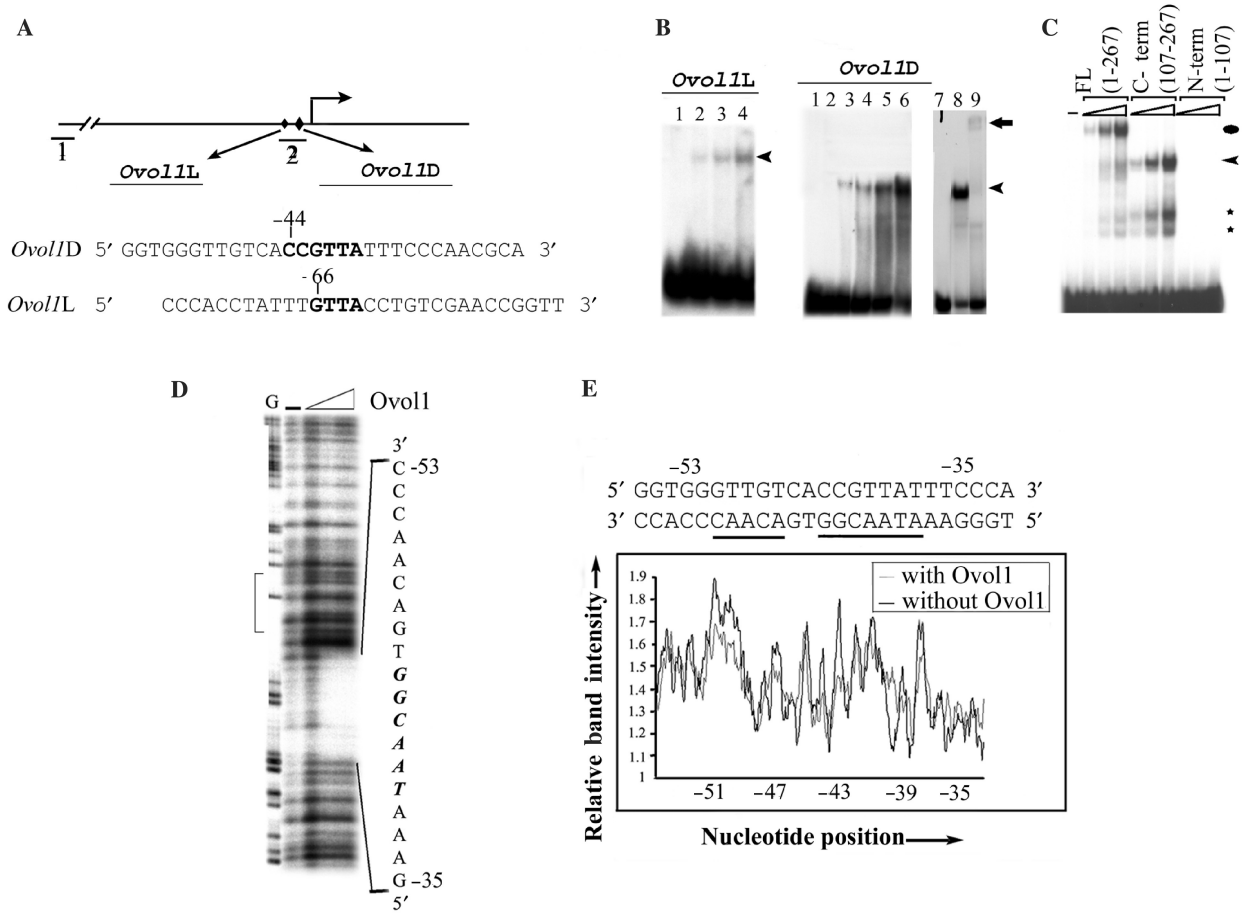

Figure 1. Ovol1 binds to its own promoter and binding requires the zinc finger domain. (**A**) Organization of the *Ovol1* promoter showing the positions of the proximal (*Ovol1D*) and distal (*Ovol1L*) sites, with their sequences shown below the stick diagram. The transcription start site is +1. Also indicated are the positions of primer sets 1 and 2 used for ChIP assays (see below). (**B**) Results of EMSA assays showing binding of recombinant Ovol1 to CCGTTA-containing oligonucleotides *Ovol1L* (left) and *Ovol1D* (right). Left panel: lane 1, free probe, lanes 2–4, with increasing amounts (172–688 nM) of recombinant His_6–Ovol1. Right panel: lanes 1 and 7, free probe; lanes 2–6, with increasing concentrations, (50–431 nM) of recombinant His_6–Ovol1; lanes 8 and 9, with 156 nM recombinant His_6–Ovol1 and with and without anti-Ovol1 antibody, respectively. Arrowhead and arrow represent Ovol1–DNA and Ovol1–DNA–antibody complexes, respectively. (**C**) Results of EMSA assays on *Ovol1D* using recombinant full-length and truncated Ovol1 proteins. Oval and arrowhead represent full-length and C-terminal Ovol1–DNA complexes, respectively. Lower bands (indicated by *) are likely due to incompletely translated protein products. (**D**) DNase1 footprint of the *Ovol1* promoter. The sequence of the footprinted region (−53 to −35) is indicated on the right. The bracket on the left indicates the position of the low-affinity site which is present within the oligonucleotide *Ovol1L*. (**E**) Densitometer tracing of hydroxyl radical footprint of the *Ovol1* promoter, with the footprinted nucleotides underlined and its position indicated.

fingers to alanines (ZnFC2A), which disrupts zinc finger structure and hence DNA binding, completely abolished repression (Figure 2B). A deletion of the CCGTTA sequence (MutP-D) in *Ovol1* promoter led to a reduction in the extent of Ovol1 repression (Figure 2C), indicating that this binding site is required to mediate maximal repression. Surprisingly, a deletion of the low-affinity distal site (MutP-L) also led to reduced repression. Moreover, a further reduction was observed when both sites were deleted (MutP-LD), suggesting an additive effect. Therefore, inside the cells both the high- and low-affinity sites are utilized for repression. Collectively, these studies, while indicative of a somewhat promiscuous nature of DNA sequence recognition of Ovol1 within cells, demonstrate that Ovol1 represses the basal transcription of *Ovol1* promoter by directly binding to it.

Ovol1 competes with c-Myb for DNA binding and represses c-Myb-activated transcription

Interestingly, the CCGTTA sequence to which Ovol1 binds is identical to the high-affinity binding site of c-Myb, a proto-oncoprotein and transcription activator (23,30–33). This finding raises the possibility that Ovol1

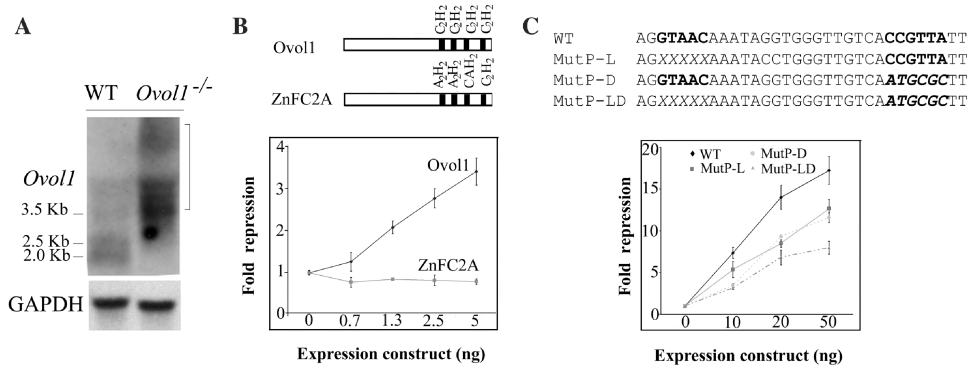

Figure 2. Ovol1 represses its own transcription. (**A**) Results of northern blot analysis of E16.5 wild-type and *Ovol1*$^{-/-}$ skin. The *Ovol1* probe detects transcripts of expected sizes in the wild type (7). The bracket indicates high-molecular-weight gene products of the mutant *Ovol1* locus. The level of GAPDH serves as a loading control. Multiple embryos per genotype were examined and representative results are shown. (**B**) Ovol1 represses *Ovol1* promoter in a DNA binding-dependent manner. The exact mutations made in ZnFC2A are indicated. Concentrations of expression constructs are: Ovol1—0.7, 1.3, 2.5 and 5 ng; ZnFC2A—5, 10, 15, and 20 ng. (**C**) Ovol1 repression of the *Ovol1* promoter requires both the proximal and distal sites. The sequences of wild-type and mutant promoters are as indicated at the top.

may repress transcription by competing with c-Myb for DNA binding. This biochemical model is consistent with the growth inhibitory function of Ovol1 and a role for c-Myb in maintaining immature, proliferating cells of the hematopoeitic and possibly epithelial lineages (23,34). To test this model, we first examined whether recombinant Ovol1 binds to previously reported c-Myb cognate sequences. Oligonucleotide *mim*-A contains a CCGTTA motif and hence is a high-affinity c-Myb site, whereas *mim*-C represents a low-affinity c-Myb site (32). In EMSA assays, recombinant Ovol1 bound to *mim*-A but not *mim*-C (Figure 3A). We next tested whether Ovol1 competes with c-Myb for binding to *mim*-A. The addition of increasing concentrations of recombinant Ovol1 at a fixed concentration of c-Myb resulted in a gradual decrease in the amount of c-Myb–DNA complexes and a concomitant increase in slow-migrating complexes, the mobility of which are consistent with that of Ovol1–DNA complexes (Figure 3B, lanes 1–5, and data not shown). The addition of anti-Ovol1 antibody led to a supershift of the Ovol1–DNA complexes and reappearance of the c-Myb–DNA complexes. We also found that c-Myb was able to bind to *Ovol1D*, an Ovol1 cognate sequence as shown above, and that recombinant Ovol1 competed away this binding (data not shown). Taken together, these results suggest that Ovol1 and c-Myb recognize similar DNA sequences, namely a CCGTTA motif, and that *in vitro*, Ovol1 is able to compete with c-Myb for binding to this motif.

To determine if competition for DNA binding also occurs within cells at the endogenous *Ovol1* promoter in its chromatin context, we performed chromatin immunoprecipitation (ChIP) assays on cells transfected with either c-Myb expression construct alone or both c-Myb and Ovol1 expression constructs. NIH3T3 cells instead of 293T cells were used for these experiments because they do not express any detectable levels of endogenous Ovol1 protein (data not shown), therefore allowing us to determine the competition effect of ectopically expressed Ovol1. When only c-Myb was present, we detected c-Myb occupancy at the *Ovol1* promoter in a region that contains the Ovol1/c-Myb-binding sites identified *in vitro* (amplified by primer set 2, the position of which is indicated in Figure 1A), but not the control region that is 2 kb upstream (amplified by primer set 1) (Figure 3C). When Ovol1 was introduced, however, Ovol1 but not c-Myb now occupied the *Ovol1* promoter. This result demonstrates that Ovol1, when present, displaces c-Myb from the Ovol1/c-Myb-binding sites in the endogenous *Ovol1* promoter. In contrast to wild-type Ovol1, the DNA-binding mutant, ZnFC2A, did not efficiently displace c-Myb, indicating that this ability to compete away c-Myb binding requires the DNA-binding ability of Ovol1.

The binding of c-Myb to *Ovol1* promoter raises the issue of whether c-Myb activates this promoter, since c-Myb is known to be a transcriptional activator (23). In reporter assays, c-Myb indeed activated the *Ovol1* promoter in a dosage-dependent manner (Figure 3D). Moreover, maximum activation was dependent on both the proximal CCGTTA-containing and the distal low-affinity Ovol1-binding sites (Figure 3D and data not shown). Thus, within cells, c-Myb displays identical and similarly promiscuous DNA sequence preferences as Ovol1 (see Discussion), but shows opposite transcriptional regulatory activity. To elucidate the functional consequence of Ovol1 competition with c-Myb, we set out to determine if Ovol1 represses c-Myb-activated promoter activity. Transient transfection experiments were performed using a fixed concentration (50 ng) of the c-Myb expression construct (where a ~2-fold

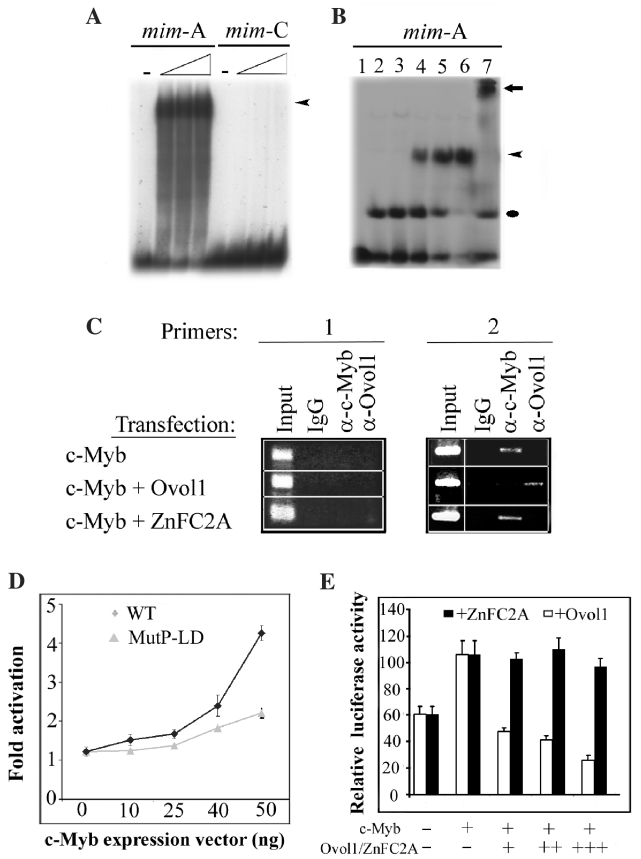

Figure 3. Ovol1 competes with c-Myb for DNA binding and represses c-Myb-activated promoter activity. (**A**) Results of EMSA assays showing that Ovol1 binds to c-Myb cognate site *mim-A* but not *mim-C* (for oligonucleotide sequences, see Materials and Methods). '-', no protein. ▷ represents increasing concentrations (216–650 nM) of recombinant Ovol1 protein. (**B**) Ovol1 competes with c-Myb for *in vitro* interaction with *mim-A*. Lane 1, free probe; lane 2, 0.8 μg of c-Myb bacterial extract; lanes 3–6, 0.8 μg c-Myb extract and increasing concentrations (31–188 nM) of recombinant Ovol1 protein; lane 7, 0.8 μg c-Myb extract + recombinant Ovol1 (188 nM) + anti-Ovol1 antibody. Oval, arrowhead and arrow represent c-Myb–DNA, Ovol1–DNA and Ovol1–DNA–antibody complexes, respectively. (**C**) Results of ChIP assays showing that Ovol1 competes with c-Myb for binding to the endogenous *Ovol1* promoter. Equivalent levels of Ovol1 and ZnFC2A proteins were expressed (data not shown). (**D**) c-Myb activates the *Ovol1* promoter in an Ovol1-binding site-dependent manner. (**E**) Ovol1 represses c-Myb-activated *Ovol1* promoter activity in a DNA binding-dependent manner.

activation was seen) and increasing concentrations of the Ovol1 expression construct. A dosage-dependent repression was observed; at high concentrations Ovol1 repressed the promoter to a level that is well below the basal activity (Figure 3E). When ZnFC2A was used instead of the wild type, a complete loss of repression was observed. Therefore, Ovol1 represses both basal and c-Myb-activated transcription of the *Ovol1* promoter, and at least one underlying mechanism of this repression is the displacement of c-Myb from its cognate sites, thereby antagonizing c-Myb activation.

Ovol1 represses basal and activated transcription of the *Ovol1* promoter by recruiting HDAC activity via its SNAG domain

Sequence analysis of the Ovol1 protein revealed the presence of an N-terminal 9-amino acid SNAG domain (Figure 4A), which was first identified in proto-oncoprotein Gfi-1 and vertebrate Snail-related proteins (9). Since the SNAG domain has been functionally implicated in recruiting HDAC1 and –2 (35,36), we hypothesized that Ovol1 may also repress transcription actively, namely by recruiting HDAC co-repressors. A generally accepted criterion for an active repressor is that it can repress transcription independently of its own DNA recognition context (37). Indeed, Ovol1 when fused to a Gal4 DNA-binding domain (Gal4DBD) was able to repress the Gal-tk promoter, where the minimum tk promoter is under the control of multimerized Gal4-binding sites (38), whereas GalDBD alone had no effect (Figure 4A and data not shown). Subsequent deletion studies mapped the repression domain to an N-terminal 45-amino-acid region encompassing the SNAG domain (data not shown). To determine if the SNAG domain is indeed required for auto-repression, we generated untagged Ovol1 mutant derivatives containing deletion of (Δ15 and Δ6SNAG), or a point mutation (P2ASNAG) in SNAG, and assayed their repressor activity on the *Ovol1* promoter. These mutations led to a complete loss of repression, while the wild-type protein of comparable expression levels repressed efficiently (Figure 4B). These results indicate that SNAG is essential for Ovol1 repression of the basal activity of *Ovol1* promoter. It is unlikely that the SNAG in Ovol1 is involved in DNA binding or nuclear localization, as we have shown that the N-terminal half of Ovol1 is dispensable for DNA binding (see above), and that Δ15 was properly localized to the cell nuclei (data not shown).

We next directly investigated whether Ovol1 repression of its own promoter is HDAC-dependent. As observed in Figure 4C, TSA treatment did not significantly affect the basal activity of *Ovol1* promoter but led to a significant reduction (~4-fold) in repression by Ovol1. Having established that Ovol1 repression requires HDAC activity, we next performed immmunoprecipitation (IP) assays to determine if Ovol1 interacts with HDACs. Indeed, Ovol1 protein was immunoprecipitated from extracts of 293T cells transfected with Flag-tagged HDAC1 by an anti-Flag antibody, but not by the appropriate IgG control (Figure 4D). Conversely, anti-Ovol1 antibody but not the relevant IgG control immunoprecipitated both exogenously and endogenously expressed HDAC1. In contrast, the anti-Flag antibody did not efficiently immunoprecipitate the Δ15 protein that lacks the SNAG domain. Therefore, the SNAG domain, which mediates maximum Ovol1 repression, is also required for its optimum

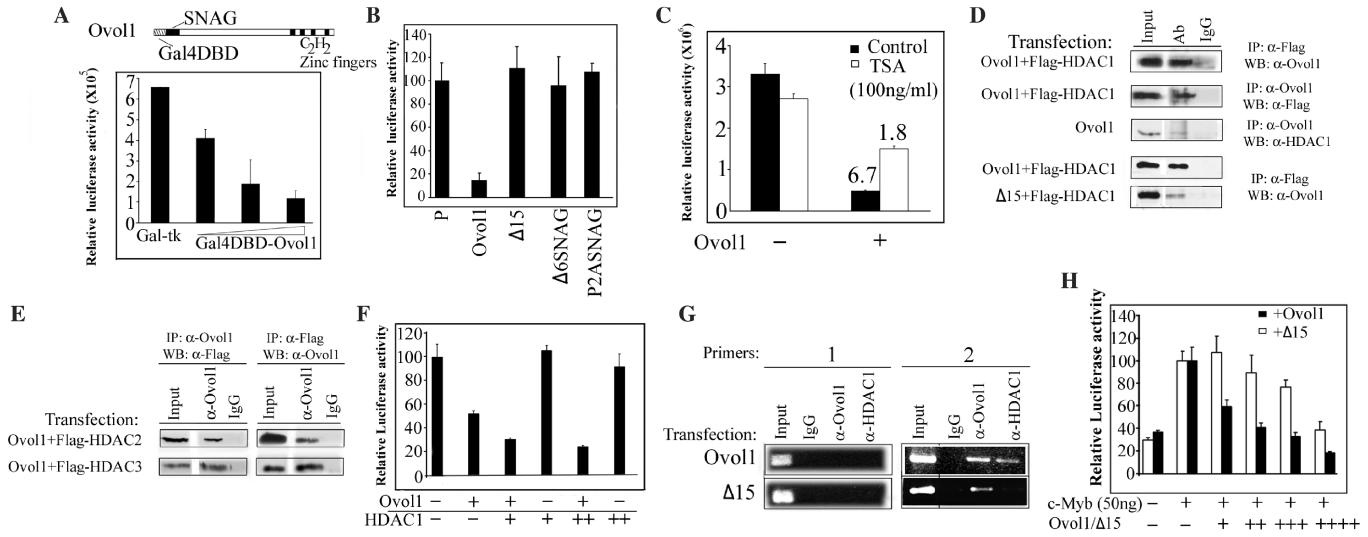

Figure 4. Ovol1 repression requires the SNAG domain and its HDAC interaction. (**A**) Ovol1 represses transcription when tethered to heterologous DNA. (**B**) Disruption of the SNAG domain abolishes Ovol1 repression of its own promoter. P, promoter only. Δ15, a truncated protein lacking the first 15 amino acids including the SNAG domain. Δ6SNAG, a protein where six of the nine core amino acids of SNAG are deleted. P2ASNAG, a protein where the highly conserved proline residue at position 2 (22) is replaced by an alanine. (**C**) Reduced repression upon TSA treatment suggests that Ovol1-mediated repression is HDAC-dependent. The numeric values above the bars represent the actual extent of repression by Ovol1 in the absence (control) or presence of TSA. (**D**) Ovol1 interacts with HDAC1 via its SNAG domain. The antibodies (Ab) used for IP and Western are indicated on the right. IgG, control immunoglobulin. (**E**) Ovol1 interacts with HDAC2 and −3. (**F**) HDAC1 augments Ovol1-mediated repression of the *Ovol1* promoter. (**G**) Results of ChIP assays revealing Ovol1 and HDAC1 occupancy at the endogenous *Ovol1* promoter in a region containing Ovol1-binding sites. For positions of primer sets, see Figure 1A. (**H**) Inability of Ovol1 to interact with HDAC1 (Δ15) results in compromised repression of c-Myb-activated transcription.

interaction with HDAC1. Interestingly, while we also observed interaction of Ovol1 with HDAC2 and −3, no apparent interaction with the mSin3A co-repressor was detected (Figure 4E and data not shown). This finding is distinct from those made for Snail (35), suggesting that while the SNAG domain in both Ovol1 and Snail proteins is involved in interaction with HDAC co-repressor complexes, the exact nature/composition of the complexes is protein specific. To further demonstrate a functional involvement of HDACs in Ovol1 repression, we co-transfected increasing amounts of an HDAC1 expression plasmid along with the Ovol1 expression construct. Indeed, an HDAC1 dosage-dependent enhancement of promoter repression was observed (Figure 4F). This enhancement required the presence of Ovol1, suggesting that HDAC1 is recruited to the promoter via Ovol1.

We next performed ChIP assays to directly examine the recruitment of HDAC1 by Ovol1 to the promoter in its genomic context. Consistent with the results described above, both wild-type and Δ15 Ovol1 proteins were recruited to the *Ovol1* promoter in a region that contains the Ovol1-binding sites, whereas no association was observed in the control region (Figure 4G). However, HDAC1 occupied the same region only when wild-type Ovol1 was present. These results indicate that HDAC1 is recruited to Ovol1 sites that are present in the genomic *Ovol1* locus, and that the SNAG domain of Ovol1 is responsible for HDAC1 recruitment. Collectively, our studies provide strong evidence that Ovol1 is able to actively repress the transcription of *Ovol1* promoter, likely by recruiting HDAC activity to its target sites.

To address the relative contribution of passive and active repression mechanisms in c-Myb-activated transcription, we compared the dosage effect of wild-type and Δ15 Ovol1. Since Δ15 is deficient in HDAC1 interaction but is able to bind DNA, we predicted that its repression of the *Ovol1* promoter is indicative of the extent of passive repression, and would therefore be less dramatic than the wild type. Indeed, at high concentrations, wild-type Ovol1 repressed c-Myb-activated transcription to an extent that is below the basal level, whereas Δ15 was only able to bring the promoter activity back down to the basal level (Figure 4H). This result suggests that Ovol1 not only displaces c-Myb to release activation, but also recruits HDAC activity to bring about additional repression at the same time. Therefore, Ovol1 combines passive and active repression mechanisms to achieve maximum repression of the *Ovol1* promoter.

Ovol1 and c-Myb exert opposing effects on histone H3 acetylation at the *Ovol1* promoter

HDACs repress transcription by deacetylating histone tails at the target promoter, whereas c-Myb is known to activate transcription by acetylating histones at its target promoters via interaction with the histone acetyl transferase (HAT) p300 (39). We therefore hypothesized that the

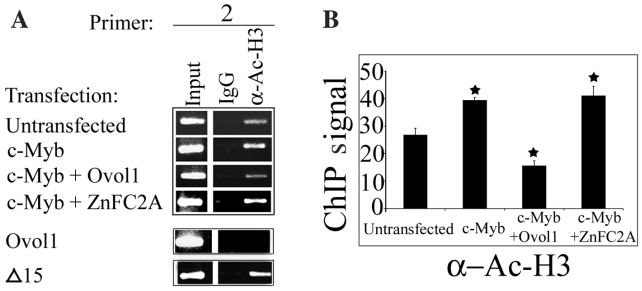

Figure 5. Opposing effects of Ovol1 and c-Myb on histone H3 acetylation at the endogenous *Ovol1* promoter. (**A**) Results of ChIP assays showing that c-Myb and Ovol1 occupancy correlates with increased and decreased respectively histone H3 acetylation from the basal level. (**B**) Results of quantification of ChIP signals. Error bars were calculated from three independent PCR reactions of a single immunoprecipitate, and results are representative of multiple ChIP experiments. '*' indicates statistically significant ($P<0.003$) difference from the untransfected sample.

switch in promoter occupancy from c-Myb to Ovol1 leads to a HAT-HDAC switch, thereby resulting in a deacetylated chromatin to silence gene expression. To test this model, we examined if changes in Ovol1 and c-Myb occupancy affects histone H3 acetylation at the *Ovol1* promoter. Upon transfection with c-Myb, a slight but reproducible increase in H3 acetylation was detected in the region that contains Ovol1/c-Myb-binding sites (Figure 5A and B), supporting the previous report that c-Myb facilitates H3 acetylation at its target promoter (39). In contrast, when Ovol1 alone was transfected, a reduction in H3 acetylation was seen, and the reduction depended on the presence of the first 15 amino acids of the protein (Figure 5A). Based on this result and studies presented above, we surmise that the SNAG domain is a key in recruiting HDAC1, which in turn deacetylates histone H3 at the target chromatin. When Ovol1 and c-Myb were co-introduced, the level of acetylated H3 at the promoter was now significantly lower than that with only c-Myb, and was comparable to that with only Ovol1 (Figure 5A and B). Co-introduction of ZnFC2A with c-Myb however, failed to reduce the c-Myb-enhanced H3 acetylation, indicating that binding of Ovol1 to the promoter is required for the observed reduction in histone acetylation levels. These differences between various conditions were reproducible and statistically significant. In all experiments, no change in H3 acetylation of the control region was observed (data not shown). Collectively, our data suggest that in cells, Ovol1 not only displaces c-Myb, hence decreasing c-Myb-facilitated histone acetylation, but also recruits HDAC activity to decrease the basal level of histone acetylation at the promoter.

DISCUSSION

Auto-regulation is a well-known mechanism to intricately regulate the concentration of developmentally important transcription factors, and known examples include Snail1 and Gfi-1B repressors (40–43). The idea of a negative auto-regulation of *Ovol1* is supported by our *in vivo* studies detecting increased levels of *Ovol1* transcripts in tissues where Ovol1 protein production is ablated, and by our *in vitro* studies that Ovol1 binds to and represses its own promoter. Our study, in light of previous reports on *Drosophila ovo* (12,13), suggests that auto-regulation is an evolutionarily conserved aspect of *Drosophila* and mouse *ovo* genes.

To date, studies on *ovo* genes have focused on their biological function and genetic context. Our work is the first to probe into the biochemical mechanisms by which this family of zinc finger proteins regulates transcription. Our results demonstrate that Ovol1 represses basal transcription in a manner that depends on its N-terminal SNAG moiety. The SNAG domain is found in multiple transcriptional repressors, where both its sequence and position are conserved (36,44). Our result that SNAG is important for Ovol1 repression is consistent with previous reports demonstrating a functional involvement of SNAG in other repressors including Gfi-1 and Snail (35,36). The N-terminal location of the SNAG domain is likely important for its repressive function, as Ovol1 protein tagged at the N-terminus does not repress as well as the untagged protein (data not shown). Ovol1 is also capable of repressing activated transcription by competing with the c-Myb activator for binding to common DNA sites. Taken together, our data suggest a novel model where Ovol1 uses an active repression mechanism to repress basal transcription of its promoter, and uses both passive and active repression mechanisms in combination to exert maximum repression of c-Myb-activated transcription (Figure 6). A functional outcome of the c-Myb-Ovol1 switch at the target promoter is the change from an acetylated, presumably open chromatin, to a deacetylated, presumably condensed chromatin, resulting in silencing of target gene expression. Although not proven, dual (active and passive) repression has been implicated for vertebrate members of the Snail family of zinc finger repressors, which are involved in important developmental processes such as mesoderm and neural crest formation [reviewed in (44)]. While a SNAG domain is found in all vertebrate but not the *Drosophila* members of the Snail protein family (36), a domain bearing resemblance to SNAG consensus is present at the N-termini of mouse Ovol2, human Ovol1 and Ovol2, as well as *Drosophila* Svb, an epidermis-specific Ovo protein isoform (45). The significance of this domain in the biochemical activities of these other Ovo proteins remains to be addressed. The similarity between Ovol1 and Snail1 repressors in auto-regulation and mode of repression is intriguing. In fact, Ovol1 shares a 28% sequence identity (39% similarity) (including SNAG domain) with the mouse Snail1 protein. A negative feedback loop to self-limit expression and dual repression to ensure an efficient, activation-silencing switch might be

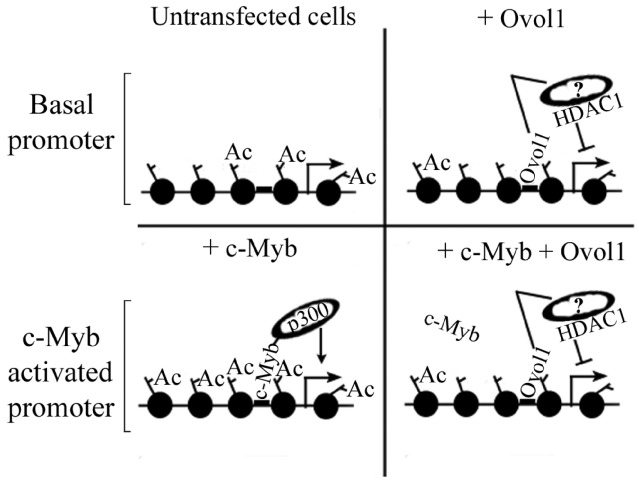

Figure 6. Working model of passive and active repression by Ovol1. Ovol1 recruits to its own promoter HDAC-containing co-repressor complexes, which in turn deacetylates histones at the chromatin, resulting in silencing of basal transcription (top right). c-Myb, via binding to the same DNA sequences, recruits p300 HAT, which in turn acetylates histones at the chromatin, resulting in gene activation (bottom left). Ovol1 is able to repress activated transcription to below-basal level by displacing c-Myb (passive) from and by recruiting HDAC co-repressor complexes (active) to its own promoter, thereby silencing activated transcription (bottom right).

necessary for developmentally important repressors to regulate cell fates at important crossroads such as proliferation and terminal differentiation.

In addition to HDAC1, Ovol1 also interacts with two other Class I HDACs, HDAC2 and -3, but not with co-repressor mSin3A. This differs from previous studies on Snail, where the SNAG domain interacts with HDAC1, -2 and mSin3A but not HDAC3 (35). It has been suggested that the Snail protein might assemble both mSin3A-dependent and -independent co-repressor complexes (35). Our studies on Ovol1 provide yet another possibility for SNAG-mediated complex formation, and extend our understanding of the repertoire of HDAC-containing co-repressor complexes. This work now adds Ovol1 to the list of versatile transcriptional repressors that can repress transcription in multiple ways.

We have recently shown that Ovol1 represses c-Myc and Id2 transcription by binding to their promoters (8,9). c-Myc is a known target of c-Myb (46–48), and our DNA-binding studies have shown that c-Myb indeed binds to an Ovol1 site in the Id2 promoter (data not shown). Therefore, the passive and active repression mechanisms of Ovol1 discovered here may apply to Ovol1-mediated regulation of its other target genes. In addition to discovering the CCGTTA-containing high-affinity site, this article and our previous work also identified atypical Ovol1-responsive elements that show low-binding affinity *in vitro* but are utilized inside cells (9). This extends the parallel with c-Myb, as it was previously reported that low-affinity c-Myb-binding sites are indeed functionally utilized (46,47). Alternative mechanisms such as assistance from auxiliary factors might exist to recruit the proteins to these sites *in vivo*. Systematic ChIP-on-chip analysis of Ovol1 binding *in vivo* might reveal additional atypical sites and shed light on the underlying mechanisms. The discovery of competition between Ovol1 and c-Myb in DNA binding and transcriptional regulation is particularly exciting in light of their apparently opposing biological functions. c-Myb positively regulates the proliferation of immature cells that are committed to differentiation (23), while Ovol1 is expressed later in a differentiation pathway and is necessary for efficient proliferation arrest (7–9,15). Based on the data presented here, it is tempting to speculate that c-Myb and Ovol1 transcriptional regulation represent two consecutive steps in a relevant differentiation pathway, where the balance of the opposing effects of these two proteins coordinates proliferation with differentiation. Since c-Myb is expressed in proliferating epidermal cells (34), a possible scenario in skin epidermis is that c-Myb activates genes such as c-Myc and Id2 to up-regulate the transient proliferation of progenitor cells that have committed to differentiate, but also turns on the expression of its own antagonist, Ovol1, to restrict proliferation to allow terminal differentiation to actually occur. This notion can now be tested using a keratinocyte differentiation as well as animal models. Since c-Myb knockout mice die during gestation prior to the onset of epidermal differentiation, a study of an epidermal involvement of c-Myb awaits the generation of a conditional allele.

ACKNOWLEDGEMENTS

We thank Kristin Brevik Andersson for c-MybR2R3 and pEQP2-CMV-c-Myb constructs and Edward Seto for Flag-tagged HDAC1, -2 and -3 constructs. We extend our thanks to Timothy Osborne, Bogi Anderson and Bruce Blumberg, for constructs used in the Gal4 system. We are immensely grateful to Mary Bennett for technical suggestions and Shannon Jessen for critical reading of the manuscript. This work was supported by NIH Grants R01-AR47320 and K02-AR51482 awarded to X.D., and M.N. was partially supported by an institutional pre-doctoral NIH Training Program in Developmental Mechanisms Underlying Congenital Defects. Funding to pay the Open Access publication charge was provided by R01-AR47320.

Conflict of interest statement. None declared.

REFERENCES

1. Li,B., Mackay,D.R., Dai,Q., Li,T.W.H., Nair,M., Fallahi,M., Schonbaum,C., Fantes,J., Mahowald,A. *et al.* (2002) The LEF1/β-catenin complex activates *movo1*, a mouse homolog of *Drosophila ovo* gene required for epidermal appendage differentiation. *Proc. Natl. Acad. Sci. U.S.A.*, **99**, 6064–6069.
2. Payre,F., Vincent,A. and Carreno,S. (1999) ovo/svb integrates Wingless and DER pathways to control epidermis differentiation. *Nature*, **400**, 271–275.
3. Mackay,D.R., Hu,M., Li,B., Rheaume,C. and Dai,X. (2006) The mouse Ovol2 gene is required for cranial neural tube development. *Dev. Biol.*, **291**, 38–52.
4. Johnson,A.D., Fitzsimmons,D., Hagman,J. and Chamberlin,H.M. (2001) EGL-38 Pax regulates the ovo-related gene lin-48 during Caenorhabditis elegans organ development. *Development*, **128**, 2857–2865.

5. Mevel-Ninio,M., Terracol,R. and Kafatos,F.C. (1991) The ovo gene of Drosophila encodes a zinc finger protein required for female germ line development. *EMBO J.*, **10**, 2259–2266.
6. Oliver,B., Perrimon,N. and Mahowald,A.P. (1987) The ovo locus is required for sex-specific germ line maintenance in Drosophila. *Genes Dev.*, **1**, 913–923.
7. Dai,X., Schonbaum,C., Degenstein,L., Bai,W., Mahowald,A. and Fuchs,E. (1998) The ovo gene required for cuticle formation and oogenesis in flies is involved in hair formation and spermatogenesis in mice. *Genes Dev.*, **12**, 3452–3463.
8. Li,B., Nair,M., Mackay,D.R., Bilanchone,V., Hu,M., Fallahi,M., Song,H., Dai,Q., Cohen,P.E. *et al.* (2005) Ovol1 regulates meiotic pachytene progression during spermatogenesis by repressing Id2 expression. *Development*, **132**, 1463–1473.
9. Nair,M., Teng,A., Bilanchone,V., Agrawal,A., Li,B. and Dai,X. (2006) Ovol1 regulates the growth arrest of embryonic epidermal progenitor cells and represses c-myc transcription. *J. Cell. Biol.*, **173**, 253–264.
10. Teng,A., Nair,M., Wells,J., Segre,J.A. and Dai,X. (2007) Strain-dependent perinatal lethality of Ovol1-deficient mice and identification of Ovol2 as a downstream target of Ovol1 in skin epidermis. *Biochim. Biophys. Acta*, **1772**, 89–95.
11. Delmas,P., Padilla,F., Osorio,N., Coste,B., Raoux,M. and Crest,M. (2004) Polycystins, calcium signaling, and human diseases. *Biochem. Biophys. Res. Commun.*, **322**, 1374–1383.
12. Lu,J., Andrews,J., Pauli,D. and Oliver,B. (1998) Drosophila OVO zinc-finger protein regulates ovo and ovarian tumor target promoters. *Dev. Genes Evol.*, **208**, 213–222.
13. Oliver,B., Singer,J., Laget,V., Pennetta,G. and Pauli,D. (1994) Function of Drosophila ovo+ in germ-line sex determination depends on X-chromosome number. *Development*, **120**, 3185–3195.
14. Unezaki,S., Nishizawa,M., Okuda-Ashitaka,E., Masu,Y., Mukai,M., Kobayashi,S., Sawamoto,K., Okano,H. and Ito,S. (2004) Characterization of the isoforms of MOVO zinc finger protein, a mouse homologue of Drosophila Ovo, as transcription factors. *Gene*, **336**, 47–58.
15. Li,B., Dai,Q., Li,L., Nair,M., Mackay,D. and Dai,X. (2002) Ovol2, a mammalian homolog of drosophila ovo: gene structure, chromosomal mapping, and aberrant expression in blind-sterile mice. *Genomics*, **80**, 319.
16. Andrews,J., Garcia-Estefania,D., Delon,I., Lu,J., Mevel-Ninio,M., Spierer,A., Payre,F., Pauli,D. and Oliver,B. (2000) OVO transcription factors function antagonistically in the Drosophila female germline. *Development*, **127**, 881–892.
17. Burke,L.J. and Baniahmad,A. (2000) Co-repressors 2000. *FASEB J.*, **14**, 1876–1888.
18. Thiel,G., Lietz,M. and Hohl,M. (2004) How mammalian transcriptional repressors work. *Eur. J. Biochem.*, **271**, 2855–2862.
19. Verdin,E., Dequiedt,F. and Kasler,H.G. (2003) Class II histone deacetylases: versatile regulators. *Trends Genet.*, **19**, 286–293.
20. Johnson,A.D. (1995) The price of repression. *Cell*, **81**, 655–658.
21. Jamin,N., Gabrielsen,O.S., Gilles,N., Lirsac,P.N. and Toma,F. (1993) Secondary structure of the DNA-binding domain of the c-Myb oncoprotein in solution. A multidimensional double and triple heteronuclear NMR study. *Eur. J. Biochem.*, **216**, 147–154.
22. Gabrielsen,O.S., Sentenac,A. and Fromageot,P. (1991) Specific DNA binding by c-Myb: evidence for a double helix-turn-helix-related motif. *Science*, **253**, 1140–1143.
23. Oh,I.H. and Reddy,E.P. (1999) The myb gene family in cell growth, differentiation and apoptosis. *Oncogene*, **18**, 3017–3033.
24. Tullius,T.D. (1988) DNA footprinting with hydroxyl radical. *Nature*, **332**, 663–664.
25. Pear,W.S., Nolan,G.P., Scott,M.L. and Baltimore,D. (1993) Production of high-titer helper-free retroviruses by transient transfection. *Proc. Natl. Acad. Sci. U.S.A.*, **90**, 8392–8396.
26. Eustice,D.C., Feldman,P.A., Colberg-Poley,A.M., Buckery,R.M. and Neubauer,R.H. (1991) A sensitive method for the detection of beta-galactosidase in transfected mammalian cells. *Biotechniques*, **11**, 739–740 742–743.
27. Khan,M.M., Nomura,T., Kim,H., Kaul,S.C., Wadhwa,R., Zhong,S., Pandolfi,P.P. and Ishii,S. (2001) PML-RARalpha alleviates the transcriptional repression mediated by tumor suppressor Rb. *J. Biol. Chem.*, **276**, 43491–43494.
28. Lee,S. and Garfinkel,M.D. (2000) Characterization of Drosophila OVO protein DNA binding specificity using random DNA oligomer selection suggests zinc finger degeneration. *Nucleic Acids Res.*, **28**, 826–834.
29. Lu,J. and Oliver,B. (2001) Drosophila OVO regulates ovarian tumor transcription by binding unusually near the transcription start site. *Development*, **128**, 1671–1686.
30. Weston,K. (1998) Myb proteins in life, death and differentiation. *Curr. Opin. Genet. Dev.*, **8**, 76–81.
31. Ness,S.A., Marknell,A. and Graf,T. (1989) The v-myb oncogene product binds to and activates the promyelocyte-specific mim-1 gene. *Cell*, **59**, 1115–1125.
32. Ramsay,R.G., Ishii,S. and Gonda,T.J. (1992) Interaction of the Myb protein with specific DNA binding sites. *J. Biol. Chem.*, **267**, 5656–5662.
33. Andersson,K.B., Berge,T., Matre,V. and Gabrielsen,O.S. (1999) Sequence selectivity of c-Myb in vivo. Resolution of a DNA target specificity paradox. *J. Biol. Chem.*, **274**, 21986–21994.
34. Ess,K.C., Witte,D.P., Bascomb,C.P. and Aronow,B.J. (1999) Diverse developing mouse lineages exhibit high-level c-Myb expression in immature cells and loss of expression upon differentiation. *Oncogene*, **18**, 1103–1111.
35. Peinado,H., Ballestar,E., Esteller,M. and Cano,A. (2004) Snail mediates E-cadherin repression by the recruitment of the Sin3A/histone deacetylase 1 (HDAC1)/HDAC2 Complex. *Mol. Cell. Biol.*, **24**, 306–319.
36. Grimes,H.L., Chan,T.O., Zweidler-McKay,P.A., Tong,B. and Tsichlis,P.N. (1996) The Gfi-1 proto-oncoprotein contains a novel transcriptional repressor domain, SNAG, and inhibits G1 arrest induced by interleukin-2 withdrawal. *Mol. Cell. Biol.*, **16**, 6263–6272.
37. Hanna-Rose,W. and Hansen,U. (1996) Active repression mechanisms of eukaryotic transcription repressors. *Trends Genet.*, **12**, 229–234.
38. Kaczynski,J., Zhang,J.S., Ellenrieder,V., Conley,A., Duenes,T., Kester,H., van Der Burg,B. and Urrutia,R. (2001) The Sp1-like protein BTEB3 inhibits transcription via the basic transcription element box by interacting with mSin3A and HDAC-1 co-repressors and competing with Sp1. *J. Biol. Chem.*, **276**, 36749–36756.
39. Mo,X., Kowenz-Leutz,E., Laumonnier,Y., Xu,H. and Leutz,A. (2005) Histone H3 tail positioning and acetylation by the c-Myb but not the v-Myb DNA-binding SANT domain. *Genes Dev.*, **19**, 2447–2457.
40. Huang,D.Y., Kuo,Y.Y. and Chang,Z.F. (2005) GATA-1 mediates auto-regulation of Gfi-1B transcription in K562 cells. *Nucleic Acids Res.*, **33**, 5331–5342.
41. Fior,R. and Henrique,D. (2005) A novel hes5/hes6 circuitry of negative regulation controls Notch activity during neurogenesis. *Dev. Biol.*, **281**, 318–333.
42. Fuse,N., Hirose,S. and Hayashi,S. (1996) Determination of wing cell fate by the escargot and snail genes in Drosophila. *Development*, **122**, 1059–1067.
43. Peiro,S., Escriva,M., Puig,I., Barbera,M.J., Dave,N., Herranz,N., Larriba,M.J., Takkunen,M., Franci,C. *et al.* (2006) Snail1 transcriptional repressor binds to its own promoter and controls its expression. *Nucleic Acids Res.*, **34**, 2077–2084.
44. Nieto,M.A. (2002) The snail superfamily of zinc-finger transcription factors. *Nat. Rev. Mol. Cell Biol.*, **3**, 155–166.
45. Delon,I., Chanut-Delalande,H. and Payre,F. (2003) The Ovo/Shavenbaby transcription factor specifies actin remodelling during epidermal differentiation in Drosophila. *Mech. Dev.*, **120**, 747–758.
46. Nakagoshi,H., Kanei-Ishii,C., Sawazaki,T., Mizuguchi,G. and Ishii,S. (1992) Transcriptional activation of the c-myc gene by the c-myb and B-myb gene products. *Oncogene*, **7**, 1233–1240.
47. Cogswell,J.P., Cogswell,P.C., Kuehl,W.M., Cuddihy,A.M., Bender,T.M., Engelke,U., Marcu,K.B. and Ting,J.P. (1993) Mechanism of c-myc regulation by c-Myb in different cell lineages. *Mol. Cell Biol.*, **13**, 2858–2869.
48. Evans,J.L., Moore,T.L., Kuehl,W.M., Bender,T. and Ting,J.P. (1990) Functional analysis of c-Myb protein in T-lymphocytic cell lines shows that it trans-activates the c-myc promoter. *Mol. Cell. Biol.*, **10**, 5747–5752.